Boltzmann Schemes for the Compressible Navier-Stokes Equations

Taku Ohwada

Department of Aeronautics and Astronautics, Graduate School of Engineering, Kyoto University, Japan

Abstract. Numerical schemes for the compressible Navier-Stokes equations (CNSE) are constructed on the basis of the kinetic equation for the Chapman-Enskog NS distribution function the macroscopic variables of which satisfy the CNSE. It is clarified from this approach that the inclusion of the collision effect in the numerical flux improves the accuracy of the scheme. Then, a practically higher order scheme for the CNSE is derived and the existing first order Boltzmann scheme for the CNSE [Chou S.Y. and Baganoff D., Journal of Comput. Phys. **130**, 217-230 (1997)] is recovered as its simplified version. The numerical computation is carried out for the CNSE derived from the BGK equation. Comparisons are made with the standard solutions for the CNSE, the results of Chou-Baganoff scheme, and the BGK solutions for small Knudsen numbers.

I INTRODUCTION

The Kinetic schemes or Boltzmann schemes for the fluiddynamic equation systems are important byproducts of kinetic theory (see e.g., Refs. [1]- [7] and the references therein). In particular, the Boltzmann scheme for the compressible Euler equations (CEE) is well known and is studied in the framework of Cauchy problem of the collisionless equation. The extension to the case of the compressible Navier-Stokes equations (CNSE) is also tackled. For example, in Chou-Baganoff scheme, [5] the local Maxwellian, which is employed as the initial data in the computation for the CEE, is replaced by the Chapman-Enskog Navier-Stokes distribution function and the numerical flux is computed by using the collisionless equation as before. It is demonstrated in the problem of normal shock wave that Chou-Baganoff scheme yields valid solutions for the CNSE. The satisfactory viscous boundary-layer profiles are obtained by the Gas Kinetic BGK scheme proposed by Prendergast and Xu [4], [7] This scheme is not based on the collisionless equation and the effect of molecular collision is taken into account in the numerical flux.

Notwithstanding the successful results, the theory of Boltzmann schemes is not very transparent because of the indirect relationship between the fluiddynamic equation system and the kinetic equation that the scheme is based on. If the scheme is constructed on the basis of the kinetic equation the corresponding macroscopic variables of which satisfy the fluiddynamic equation system, the relation to the fluiddynamic equation will become obvious by construction and the criteria of the approximation will become clear. When its simplified equation is employed in the construction of the scheme, the clear information of its intrinsic error will help avoid the meaningless approximation in the actual numerical computation. On the other hand, if we regard the Boltzmann schemes as the first step of the Boltzmann solvers to analyze the actual rarefied gas flows for small Knudsen numbers, the kinetic equation should be related to the full Boltzmann equation.

In the present paper, we will study the Boltzmann schemes for the CNSE following the above strategy. We will construct the scheme on the basis of the kinetic equation for the Chapman-Enskog Navier-Stokes distribution function the macroscopic variables of which satisfy the CNSE. In the course of the construction, the necessity of the inclusion of the collision effect for the improvement of the accuracy, which is claimed in Ref. [7], will be clarified. Then, a practically second order Boltzmann scheme for the CNSE will be obtained and Chou-Baganoff scheme will be recovered as its simplified version. Further, as a byproduct of the present study, a new second order scheme (in time) for the CEE will be obtained from the kinetic equation that has a direct relationship with the CEE.

CP585, *Rarefied Gas Dynamics: 22nd International Symposium,* edited by T. J. Bartel and M. A. Gallis

REPORT DOCUMENTATION PAGE

Form Approved OMB No. 0704-0188

1. REPORT DATE (DD-MM-YYYY)	2. REPORT TYPE	3. DATES COVERED (FROM - TO)
09-07-2000	Conference Proceedings	09-07-2000 to 14-07-2000

4. TITLE AND SUBTITLE
Boltzmann Schemes for the Compressible Navier-Stokes Equations
Unclassified

5a. CONTRACT NUMBER
5b. GRANT NUMBER
5c. PROGRAM ELEMENT NUMBER

6. AUTHOR(S)
Ohwada, Taku ;

5d. PROJECT NUMBER
5e. TASK NUMBER
5f. WORK UNIT NUMBER

7. PERFORMING ORGANIZATION NAME AND ADDRESS
Department of Aeronautics and Astronautics
Graduate School of Engineering
Kyoto University
Kyoto, Japan660-8501

8. PERFORMING ORGANIZATION REPORT NUMBER

9. SPONSORING/MONITORING AGENCY NAME AND ADDRESS
AOARD
Unit 45002
APO AP, xx96337-5002

10. SPONSOR/MONITOR'S ACRONYM(S)
11. SPONSOR/MONITOR'S REPORT NUMBER(S)

12. DISTRIBUTION/AVAILABILITY STATEMENT
APUBLIC RELEASE
,

13. SUPPLEMENTARY NOTES
See Also ADM001341, Rarefied Gas Dynamics (RGD) 22nd International Symposium held in Sydney, Australia, 9-14 July 2000.

14. ABSTRACT
Numerical schemes for the compressible Navier-Stokes equations (CNSE) are constructed on the basis of the kinetic equation for the Chapman-Enskog NS distribution function the macroscopic variables of which satisfy the CNSE. It is clarified from this approach that the inclusion of the collision effect in the numerical flux improves the accuracy of the scheme. Then, a practically higher order scheme for the CNSE is derived and the existing first order Boltzmann scheme for the CNSE [Chou S.Y. and Baganoff D., Journal of Comput. Phys. 130, 217-230 (1997)] is recovered as its simplified version. The numerical computation is carried out for the CNSE derived from the BGK equation. Comparisons are made with the standard solutions for the CNSE, the results of Chou-Baganoff scheme, and the BGK solutions for small Knudsen numbers.

15. SUBJECT TERMS

16. SECURITY CLASSIFICATION OF:			17. LIMITATION OF ABSTRACT	18. NUMBER OF PAGES	19. NAME OF RESPONSIBLE PERSON
a. REPORT	b. ABSTRACT	c. THIS PAGE	Public Release	8	Fenster, Lynn lfenster@dtic.mil
Unclassified	Unclassified	Unclassified			19b. TELEPHONE NUMBER International Area Code Area Code Telephone Number 703767-9007 DSN 427-9007

II THEORY

A Notation

The main notation employed in the present paper is as follows: L is the reference length of the system under consideration; ρ_0 is the reference density; T_0 is the reference temperature; l_0 is the mean free path of the gas molecules in the equilibrium state at rest with the density ρ_0 and temperature T_0; $\epsilon = \sqrt{\pi} l_0/(2L)$; Lx_i is the space coordinate system, $(2RT_0)^{1/2}\xi_i$ is the molecular velocity, where R is the specific gas constant; $L(2RT_0)^{-1/2}t$ is the time; $\rho_0(2RT_0)^{-3/2}f(x_i, \xi_i, t)$ is the velocity distribution function; $\rho_0\rho$, $(2RT_0)^{1/2}u_i$, T_0T, p_0P ($p_0 = R\rho_0T_0$), p_0P_{ij}, and $p_0(2RT_0)^{1/2}Q_i$ are the density, flow velocity, temperature, pressure, stress tensor, and heat flow vector of the gas, respectively.

B Chapman-Enskog expansion

The Chapman-Enskog expansion of the Boltzmann equation

$$\frac{\partial f}{\partial t} + \xi_i \frac{\partial f}{\partial x_i} = \frac{1}{\epsilon} J(f, f), \tag{1}$$

for small parameter ϵ provides the materials for the construction of our Boltzmann scheme. We briefly review this expansion according to Ref. [8].

The fluiddynamic solution of the Boltzmann equation (1) is assumed to be in the form:

$$f = f(\boldsymbol{\xi}, \boldsymbol{h}, D\boldsymbol{h}, \epsilon), \tag{2}$$

where D is the abbreviation of differential operators with respect to x_i and the vector $\boldsymbol{h}$ represents the macroscopic variables, i.e., $(h_0, h_i, h_4)=(\rho, \rho u_i, 3\rho T/2 + \rho u_j^2)$, which are defined as the products of f and collision invariants $\boldsymbol{\psi}$ ($\psi_0 = 1$, $\psi_i = \xi_i$ $(i = 1, 2, 3)$, and $\psi_4 = \xi_j^2$)

$$\boldsymbol{h} = \int_{R^3} \boldsymbol{\psi} f d\boldsymbol{\xi}. \tag{3}$$

The solution (2) depends on t and x_i only through $\boldsymbol{h}$ and its derivatives $D\boldsymbol{h}$. It is also assumed that the conservation equation system for Eq. (1) is in the form:

$$\frac{\partial \boldsymbol{h}}{\partial t} = \boldsymbol{\Phi}(\boldsymbol{h}, D\boldsymbol{h}, \epsilon). \tag{4}$$

The f and $\boldsymbol{\Phi}$ are expanded into the power series of ϵ

$$f = \sum_{k=0}^{\infty} \epsilon^k f_k(\boldsymbol{\xi}, \boldsymbol{h}, D\boldsymbol{h}), \qquad \frac{\partial \boldsymbol{h}}{\partial t} = \sum_{k=0}^{\infty} \epsilon^k \boldsymbol{\Phi}_k(\boldsymbol{h}, D\boldsymbol{h}). \tag{5}$$

The coefficients f_k $(k = 0, 1, 2, \cdots)$ are the solutions of the following integral equations:

$$0 = J(f_0, f_0), \tag{6}$$

$$\sum_{l+m=k-1} \left(\frac{\partial f_l}{\partial \boldsymbol{h}} \boldsymbol{\Phi}_m + \frac{\partial f_l}{\partial D\boldsymbol{h}} D\boldsymbol{\Phi}_m\right) + \xi_i \frac{\partial f_{k-1}}{\partial x_i} = \sum_{l+m=k} J(f_l, f_m), \quad (k \geq 1). \tag{7}$$

The sequence of integral equations are solved from the lowest order under the constrain

$$\int_{R^3} \boldsymbol{\psi} f_0 d\boldsymbol{\xi} = \boldsymbol{h}, \qquad \int_{R^3} \boldsymbol{\psi} f_k d\boldsymbol{\xi} = 0 \quad (k \geq 1). \tag{8}$$

The inhomogeneous term of integral equations (7) must satisfy the compatibility condition

$$\boldsymbol{\Phi}_{k-1} + \int_{R^3} \boldsymbol{\psi} \xi_i \frac{\partial f_{k-1}}{\partial x_i} d\boldsymbol{\xi} = 0, \tag{9}$$

which determines $\boldsymbol{\Phi}_{k-1}$.

C Distribution function for CNSE

The distribution function that yields the Navier-Stokes stress tensor and heat flow vector is given by

$$f_{CNSE} = f_0 + \epsilon f_1. \tag{10}$$

The coefficient f_0 is the local Maxwellian

$$f_0 = \frac{\rho}{(\pi T)^{3/2}} \exp(-C^2), \tag{11}$$

where $C = (C_i^2)^{1/2}$ and $C_i = (\xi_i - u_i)/T^{1/2}$. The coefficient f_1 is the solution of the linear integral equation

$$2J(f_0, f_1) = [2(C_i C_j - \frac{C^2}{3}\delta_{ij})\frac{\partial u_i}{\partial x_j} + \frac{C_i}{T^{1/2}}(C^2 - \frac{5}{2})\frac{\partial T}{\partial x_i}]f_0, \tag{12}$$

under the constrain (8). For hard-sphere molecules, f_1 is given by

$$f_1 = -\frac{1}{\rho T^{1/2}}[(C_i C_j - \frac{C^2}{3}\delta_{ij})B(C)\frac{\partial u_i}{\partial x_j} + \frac{C_i}{T^{1/2}}A(C)\frac{\partial T}{\partial x_i}]f_0(C), \tag{13}$$

where the functions $A(C)$ and $B(C)$ are studied in Refs. [9] and [10] [The function $\nu(\zeta)$ in Eqs. (A1)-(A5) of Ref. [10] should be $2\sqrt{2}\nu(\zeta)$]. For the BGK equation

$$\frac{\partial f}{\partial t} + \xi_i \frac{\partial f}{\partial x_i} = \frac{1}{\epsilon}\rho(f_0 - f), \tag{14}$$

f_1 is given by

$$f_1 = -\frac{1}{\rho}[2(C_i C_j - \frac{C^2}{3}\delta_{ij})\frac{\partial u_i}{\partial x_j} + \frac{C_i}{T^{1/2}}(C^2 - \frac{5}{2})\frac{\partial T}{\partial x_i}]f_0(C). \tag{15}$$

The truncated conservation equation system

$$\frac{\partial \boldsymbol{h}}{\partial t} = \boldsymbol{\Phi}_0 + \epsilon \boldsymbol{\Phi}_1, \tag{16}$$

is the CNSE and its explicit form is

$$\frac{\partial}{\partial t}\begin{pmatrix} \rho \\ \rho u_i \\ \rho[\frac{3}{2}T + u_k^2] \end{pmatrix} + \frac{\partial}{\partial x_j}\begin{pmatrix} \rho u_j \\ \rho u_i u_j + \frac{1}{2}P_{ij} \\ \rho[\frac{3}{2}T + u_k^2]u_j + P_{kj}u_k + Q_j \end{pmatrix} = 0, \tag{17}$$

where

$$P_{ij} = P\delta_{ij} - \gamma_1 \epsilon T^\alpha (\frac{\partial u_i}{\partial x_j} + \frac{\partial u_j}{\partial x_i} - \frac{2}{3}\frac{\partial u_k}{\partial x_k}\delta_{ij}), \qquad Q_i = -\frac{5}{4}\gamma_2 \epsilon T^\alpha \frac{\partial T}{\partial x_i}. \tag{18}$$

The γ_i and α are $\gamma_1 = 1.270042427$, $\gamma_2 = 1.922284066$, and $\alpha = 1/2$ for hard-sphere molecules and $\gamma_1 = \gamma_2 = \alpha = 1$ for the BGK equation.

D Kinetic equation for f_{CNSE}

Let us consider the f_{CNSE} the macroscopic variables of which satisfy the CNSE (16). Making use of Eq. (7), we find that f_{CNSE} satisfies

$$\frac{\partial f_{CNSE}}{\partial t} + \xi_i \frac{\partial f_{CNSE}}{\partial x_i} = \tilde{J}_{CNSE}(f_{CNSE}), \tag{19}$$

where

$$\tilde{J}_{CNSE}(f_{CNSE}) = J^1 + \tilde{R}, \tag{20}$$

$$J^n = \sum_{k=0}^{n} \epsilon^k \sum_{l+m=k+1} J(f_l, f_m), \qquad \tilde{R} = \epsilon^2 (\frac{\partial f_1}{\partial \boldsymbol{h}} \boldsymbol{\Phi}_1 + \frac{\partial f_1}{\partial \nabla \boldsymbol{h}} \nabla \boldsymbol{\Phi}_1). \tag{21}$$

The functional form of $\tilde{J}_{CNSE}(f_{CNSE})$ is given and it depends on x_i and t through the macroscopic variables for f_{CNSE} and their spatial derivatives. For general distribution function f we can define the operator $\tilde{J}_{CNSE}$ in the same way. Then, we notice that $f_{CNSE}(x_i, \xi_i, t)$ is the solution of the Cauchy problem

$$\frac{\partial f}{\partial t} + \xi_i \frac{\partial f}{\partial x_i} = \tilde{J}_{CNSE}(f), \tag{22}$$

$$f(x_i, \xi_i, 0) = f_{CNSE}(x_i, \xi_i, 0). \tag{23}$$

If the numerical scheme for the CNSE is based on the above Cauchy problem, its intrinsic error is zero. If we employ its simplified equation, the resulting scheme has the intrinsic error. Next we show the simplified equation together with its intrinsic error.

The solution of the above Cauchy problem is formally written in the integral form along its characteristic line:

$$f(\xi_i, x_i, t) = f_{CNSE}(\xi_i, x_i - t\xi_i, 0) + \int_0^t [J^1 + \tilde{R}](\xi_i, x_i - (t-\tau)\xi_i, \tau) d\tau. \tag{24}$$

Then, the macroscopic variables and their spatial derivatives $\nabla^k \boldsymbol{h}$ ($k = 0, 1, \cdots$ and ∇^0 means identity) at $t = \Delta t$ are given by

$$\begin{aligned} \nabla^k \boldsymbol{h}(x_i, \Delta t) &= Y_1 + Y_2 \\ Y_1 &= \nabla^k \int_{R^3} \boldsymbol{\psi} f_{CNSE}(\xi_i, x_i - \Delta t \xi_i, 0) d\boldsymbol{\xi} \\ Y_2 &= \nabla^k \int_{R^3} \boldsymbol{\psi} \int_0^{\Delta t} [J^1 + \tilde{R}](\xi_i, x_i - (\Delta t - \tau)\xi_i, \tau) d\tau d\boldsymbol{\xi}. \end{aligned} \tag{25}$$

The Y_2 is evaluated as follows.

$$\begin{aligned} Y_2 &= \frac{\Delta t}{2} \nabla^k \int_{R^3} \boldsymbol{\psi} \Big([J^1 + \tilde{R}](\xi_i, x_i, \Delta t) + [J^1 + \tilde{R}](\xi_i, x_i - \Delta t \xi_i, 0) \Big) d\boldsymbol{\xi} + O(\Delta t^3), \\ &= -\frac{\Delta t^2}{2} \nabla^k \frac{\partial}{\partial x_i} \int_{R^3} \boldsymbol{\psi} \xi_i [J^1 + \tilde{R}](\xi_i, x_i, 0) d\boldsymbol{\xi} + O(\Delta t^3), \end{aligned} \tag{26}$$

where the trapezoid rule and the orthogonality property $\int_{R^3} \boldsymbol{\psi} J^1 d\boldsymbol{\xi} = 0$ and $\int_{R^3} \boldsymbol{\psi} \tilde{R} d\boldsymbol{\xi} = 0$ are employed. The above evaluation indicates that the influence of the molecular collision is $O(\Delta t^2)$; the intrinsic error of the scheme based on the collisionless equation (Chou-Baganoff scheme) is $O(\Delta t^2)$ and thus it is first order accurate in time. If the term J^1 is retained, the error would be $O(\epsilon^2 \Delta t^2)$. Furthermore, if J^1 is replaced by J^0, the error would be $O(\epsilon \Delta t^2)$. The third simplified equation

$$\frac{\partial f}{\partial t} + \xi_i \frac{\partial f}{\partial x_i} = J^0, \tag{27}$$

yields the approximate solution of the CNSE, the accuracy of which is practically higher order in time as long as $\epsilon \lesssim \Delta t$.

Finally, we remark on the Boltzmann scheme for the CEE. In the construction of the first order scheme the Cauchy problem of collisionless equation from the local Maxwellian is considered. Deshpande [2] and Perthame [3] constructed the second order Boltzmann schemes for the CEE by the brilliant modification of the initial data. On the other hand, the local Maxwellian f_0 the macroscopic variables of which satisfy the CEE satisfies Eq. (27) and the intrinsic error of the scheme based on Eq. (27) is zero, which implies that the second order scheme for the CEE can also be made by modifying the kinetic equation instead of the initial data.

E NUMERICAL ART

Now, all the necessary materials are prepared. Here, we construct a Boltzmann scheme for the CNSE as the finite-volume approximation of Eq. (27). In order to avoid unessential complexity, we consider the spatially one-dimensional case; the physical quantities are independent of x_2 and x_3. At $t = 0$, the macroscopic variables $\rho(x_1, 0)$, $u_i(x_1, 0)$, and $T(x_1, 0)$ are assumed to be piecewise linear over cells $(s_{j-1/2}, s_{j+1/2})$ and the initial data $f_{CNSE}(x_1, \xi_i, 0)$ is made accordingly. Let the average of $\boldsymbol{h}(x_1, t)$ over the cell $(s_{j-1/2}, s_{j+1/2})$ be denoted by $\boldsymbol{h}_j(t)$. Multiplying Eq. (27) by $\boldsymbol{\psi}$ and integrating the result over the whole velocity space R^3, over the cell $(s_{j-1/2}, s_{j+1/2})$, and over the time interval $(0, \Delta t)$, respectively, we have

$$\boldsymbol{h}_j(\Delta t) = \boldsymbol{h}_j(0) - \frac{1}{\Delta x}(\boldsymbol{F}_{j+1/2} - \boldsymbol{F}_{j-1/2}), \tag{28}$$

where $\Delta x = s_{j+1/2} - s_{j-1/2}$ and $\boldsymbol{F}_{j\pm1/2}$ are the flux vectors given by

$$\boldsymbol{F}_{j\pm1/2} = \int_0^{\Delta t} \int_{R^3} \boldsymbol{\psi}\xi_1 f(s_{j\pm1/2}, \boldsymbol{\xi}, t) d\boldsymbol{\xi} dt. \tag{29}$$

We split the flux vector $\boldsymbol{F}_{j+1/2}$ into two parts according to the direction of characteristic line of Eq. (27):

$$\begin{aligned} \boldsymbol{F}_{j+1/2} &= \boldsymbol{F}^+_{j+1/2} + \boldsymbol{F}^-_{j+1/2}, \\ \boldsymbol{F}^\pm_{j+1/2} &= \int_0^{\Delta t} \int_{\xi_1 \gtrless 0} \xi_1 \boldsymbol{\psi} f(s_{j+1/2} \mp 0, \boldsymbol{\xi}, t) d\boldsymbol{\xi} dt, \end{aligned} \tag{30}$$

where $s_{j+1/2} + 0$ and $s_{j+1/2} - 0$ mean the limiting values; f for $s_{j+1/2} + 0$ is computed in the right cell and that for $s_{j+1/2} - 0$ is done in the left one. Recall that the intrinsic error of the scheme based on Eq. (27) is $O(\epsilon \Delta t^2)$. We can employ the approximation of the integrand:

$$f(s_{j+1/2} \mp 0, \xi_1, t) = (f_0 + \epsilon f_1)(s_{j+1/2} \mp 0, \boldsymbol{\xi}, 0) + t[J^0 - \xi_1 \frac{\partial f_0}{\partial x_1}](s_{j+1/2} \mp 0, \boldsymbol{\xi}, 0) + O(\epsilon t + t^2), \tag{31}$$

Then, we have

$$\boldsymbol{F}^\pm_{j+1/2} = \int_{\xi_1 \gtrless 0} \xi_1 \boldsymbol{\psi} \left(\Delta t (f_0 + \epsilon f_1) + \frac{\Delta t^2}{2} [J^0 - \xi_1 \frac{\partial f_0}{\partial x_1}] \right) (s_{j+1/2} \mp 0, \boldsymbol{\xi}, 0) d\boldsymbol{\xi}. \tag{32}$$

The integration with respect to $\boldsymbol{\xi}$ can be done in advance. In the case of the standard Boltzmann equation, it is convenient to employ the polynomial approximation of the functions $A(C)$ and $B(C)$ in f_1. In the case of the BGK equation, these functions are polynomials of C [see Eq. (15)]. Although the computation is tedious and the resulting expression is lengthy, however, the computer algebra, such as MATHEMATICA, is very useful and we are free from the cumbersome business.

For comparison, we present two other formulas of the numerical flux without the term J^0. The first one is

$$\boldsymbol{F}^\pm_{j+1/2} = \Delta t \int_{\xi_1 \gtrless 0} \xi_1 \boldsymbol{\psi} \left(f_0 + \epsilon f_1 \right) (s_{j+1/2} \mp 0, \boldsymbol{\xi}, 0) d\boldsymbol{\xi}, \tag{33}$$

which gives Chou-Baganoff numerical flux. The second one is

$$\boldsymbol{F}^\pm_{j+1/2} = \int_{\xi_1 \gtrless 0} \xi_1 \boldsymbol{\psi} \left(\Delta t (f_0 + \epsilon f_1) - \frac{\Delta t^2}{2} \xi_1 \frac{\partial f_0}{\partial x_1} \right) (s_{j+1/2} \mp 0, \boldsymbol{\xi}, 0) d\boldsymbol{\xi}. \tag{34}$$

This is the modified version of Chou-Baganoff numerical flux (33), where the slope in the cell is taken into account up to the order of Δt^2. For $\epsilon = 0$, the formula (34) becomes the 2nd order kinetic flux vector splitting scheme for the CEE, which is second order accurate in space but is not in time because of the lack of the term J^0. The formula (32) with $\epsilon = 0$ gives the numerical flux for the CEE, which is second order accurate in time as well as in space.

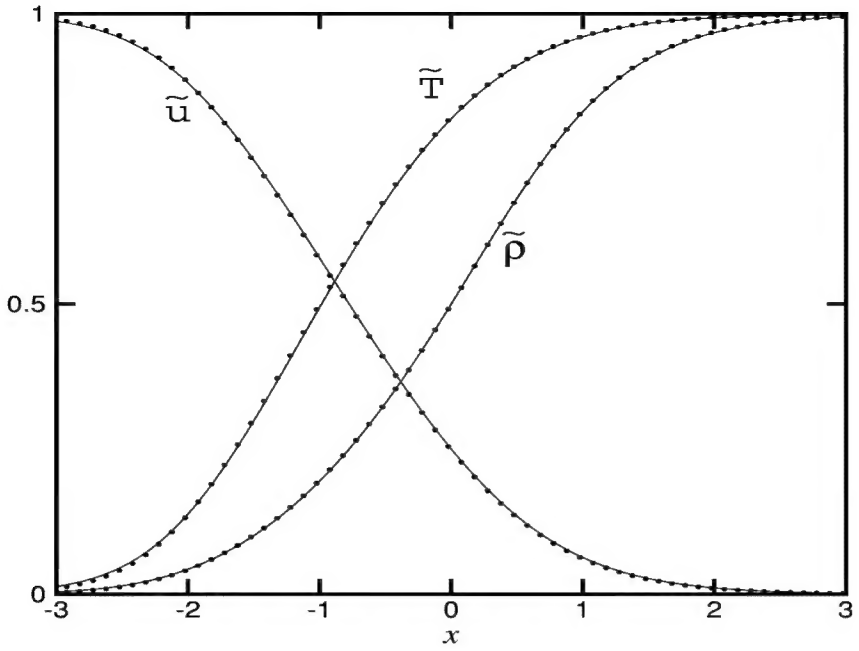

FIGURE 1. Comparison of shock profile for $M = 3$.

III NUMERICAL DEMONSTRATION

We consider the spatially one-dimensional problems of normal shock wave and plane Couette flow and carry out the computation for the CNSE derived from the BGK equation. Comparisons are made with the BGK solutions as well as the standard solution of the CNSE. In the following, the physical quantities of the gas is independent of x_2 and x_3 and x_1 will be denoted by x. In all the computations of the CNSE, $\Delta x (= s_{j+1/2} - s_{j-1/2})$ and Δt are, respectively, uniform and no slope limiter is employed.

Figure 1 shows the normalized density $\tilde{\rho}$, flow velocity $\tilde{u}$, and temperature $\tilde{T}$ in the plane shock layer at the upstream Mach number of 3 ($M = 3$). In the figure, the reference length L is equal to $\sqrt{\pi} l_0/2$ ($\epsilon = 1$) and ρ_0 and T_0 are those at upstream condition ($x = -\infty$). The symbol indicates the result of the present scheme ($\Delta x = 0.1$, and $\Delta t = 0.005$) and the solid line is the reference solution obtained by the method employed in Ref. [11]. The agreement is very satisfactory and the same observation is made for higher Mach numbers. Needless to say, the highly nonequilibrium flows is out of the application range of the CNSE and the results in the figure are not physically correct. This figure shows the validity of the present scheme as the solver for the CNSE. The leading error of the present scheme for time step Δt is $O(\epsilon \Delta t^2)$ and ϵ corresponds to the local Knudsen numeber, which is $O(1)$ in the problem of strong shock wave. Thus, in this problem the accuracy of the present scheme becomes first order.

The accuracy of the present scheme (32) is practically higher order in time as long as $\epsilon \lesssim \Delta t$. Tables 1-3 shows the result of the Cauchy problem of the CNSE with $\epsilon = 0.0001$ from the initial condition $\rho = 1$, $u_i = 0$, and $T = 1 + \exp(-x^2)$. The time step is given by $\Delta t = \Delta x/8$. For comparison the result of Chou-Baganoff scheme (33) and that of modified one (34) are tabulated in the tables. These tables indicate that the inclusion of the collision effect improves the rate of convergence greatly.

Finally we show the results of the Couette flow between two parallel plates; both plates are kept at a uniform temperature T_0; one of the plates ($x = 0$) is at rest and the other ($x = 1$) is moving at the speed of 1 (the dimensional speed is $\sqrt{2RT_0}$). Figure 2 shows the results at the Knudsen number ($= 2\epsilon/\sqrt{\pi}$) of 0.012 (based on the distance between the plates, wall temperature T_0, and the average density). In the computation of the CNSE the slip boundary condition with the slip coefficients for the BGK equation and the diffuse reflection [12]

TABLE 1. The density ρ at $(x,t) = (0.8, 2)$.

Δx	Present [Eq. (32)]	Chou-Baganoff [Eq.(33)]	Modified [Eq. (34)]
0.2	0.633401	0.631299	0.642383
0.1	0.633093	0.631932	0.637664
0.05	0.633083	0.632472	0.635384
0.025	0.633083	0.632769	0.634237

TABLE 2. The flow velocity u_1 at $(x,t) = (0.8, 2)$.

Δx	Present [Eq. (32)]	Chou-Baganoff [Eq.(33)]	Modified [Eq. (34)]
0.2	0.060357	0.054316	0.061260
0.1	0.059545	0.056383	0.060139
0.05	0.059458	0.057865	0.059770
0.025	0.059455	0.058658	0.059612

TABLE 3. The temperature T at $(x,t) = (0.8, 2)$.

Δx	Present [Eq. (32)]	Chou-Baganoff [Eq.(33)]	Modified [Eq. (34)]
0.2	1.918041	1.911346	1.898904
0.1	1.918886	1.915558	1.908888
0.05	1.918896	1.917264	1.913801
0.025	1.918887	1.918081	1.916315

is employed. The symbol of black square indicates the result of the present scheme for $(\Delta x, \Delta t) = (0.1, 0.01)$ and that of white circle does that for $(\Delta x, \Delta t) = (0.02, 0.002)$. They are compared with the solution of the BGK equation under the diffuse reflection boundary condition (solid line). It is seen that the agreement with the BGK solution is very satisfactory (the Knudsen layer correction to the CNSE solution is not made in the figure; this layer is not taken into account in the computation of the CNSE since it does not contribute to the numerical flux). Incidentally, we remark that similar observations are made in the problems of weak shock wave and nonlinear heat transfer between parallel plates for small Knudsen numbers.

In the present computation, the CNSE derived from the BGK equation is employed. The extension of the scheme to the CNSE derived from the standard Boltzmann equation can be done straightforwardly and the precise numerical computation of the standard Boltzmann equation to establish the reference solutions, though heavy, can be done at least for spatially one-dimensional case (see e.g., Refs. [13] and [14]). The extension and the numerical demonstration are in preparation.

IV CONCLUDING REMARKS

We have constructed the Boltzmann schemes for the CNSE that follow the time evolution of Chapman-Enskog NS distribution function. The agreement between the CNSE results and the BGK solutions seems to support the legitimacy of this expansion up to the Navier-Stokes level. As noted in Ref. [15], however, the solution of the CNSE is obtained by the correction to that of the CEE in this expansion. In the abovementioned problems, i.e., the plane Couette flow, weak shock, and heat transfer between parallel plates, the CEE does not yields the first order approximation (weak solutions are not considered in this expansion). These problems are out of the application range of this expansion in the strict scense. The legitimacy of the use of the CNSE in the weak shock problem is given in Refs. [16] and [13] by the systematic expansion and it is confirmed that the CNSE yields the solution correct up to $O(M-1)$. The CNSE under the slip boundary condition also yields the solution correct up to $O(\epsilon)$ in the above two-surface problems, which is verified for the first time by the systematic analysis in the framework of the boundary-value problem.

The asymptotic theory for small Knudsen numbers has made a great progress in the last three decades (see Ref. [15] and the references therein). The ghost effect is one of the most striking discoveries; in Ref. [17] the discrepancy of the CNSE in the continuum limit is revealed by the systematic analysis based on the Boltzmann equation together and its numerical demonstration. The numerical schemes for continuum gasdynamic equation systems are sometimes employed as the Boltzmann solvers for small Knudsen numbers under the seeming consistency with the old theory, which is not developed in the framework of the boundary-value problem. It

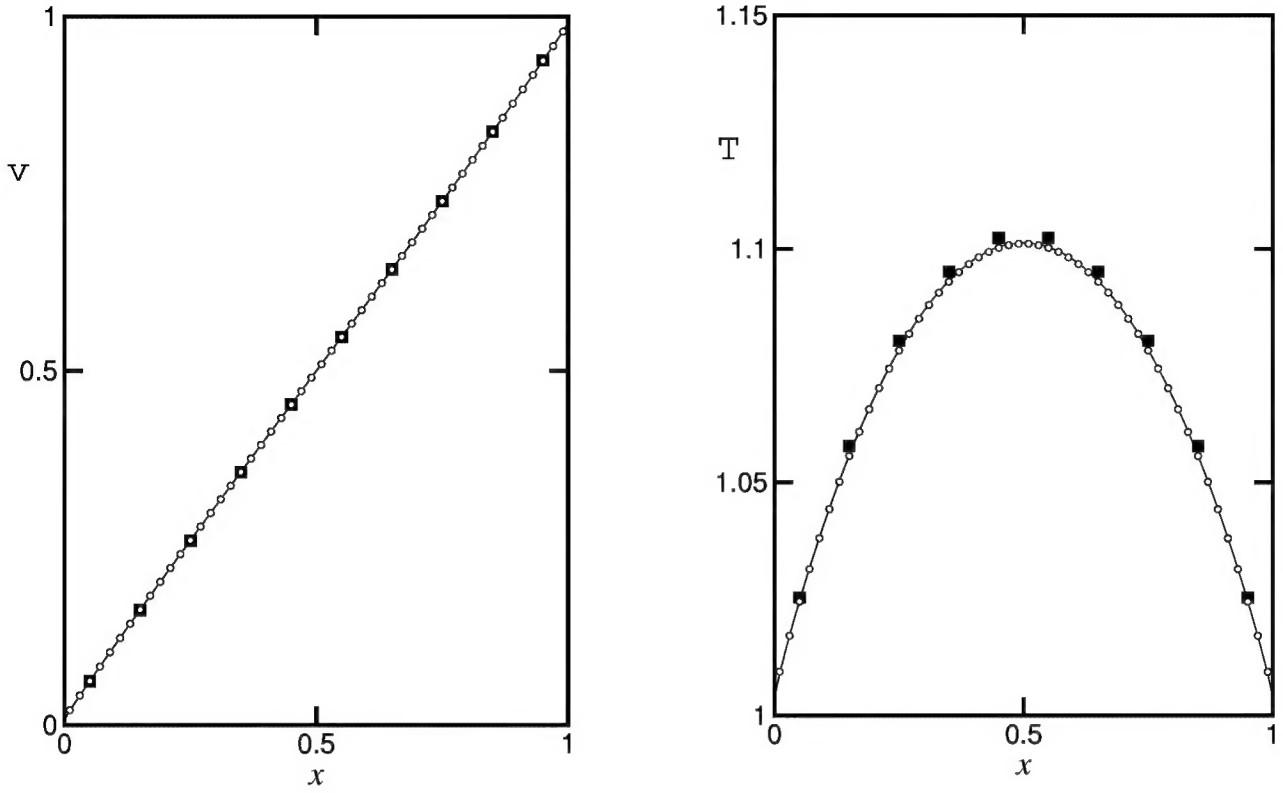

FIGURE 2. Comparison of flow velocity v and that of temperature T at Kn=0.012.

is dangerous to employ the Boltzmann schemes for this purpose without paying attention to the recent theory established by the systematic analyses.

REFERENCES

1. Pullin D., *J. Compt. Phys.* **34**, 231 (1980).
2. Deshpande S.M., *NASA Langley Tech. Paper* No. 2613 (1986).
3. Perthame B., *SIAM J. Numer. Anal.* **29**, 1 (1992).
4. Prendergast K.H. and Xu K., *J. Compt. Phys.* **109**, 53 (1993).
5. Chou S.Y. and Baganoff D., *J. Compt. Phys.* **130**, 217 (1997).
6. Moschetta, J.M. and Pullin, D., *J. Compt. Phys.* **133**, 193 (1997).
7. Xu K., *Von Karman Institute Report* 1998-03 (1998).
8. Grad H., *Handbuch der Physik*, (Springer-Verlag, Berlin, 1958), pp.205-294.
9. Pekeris C.L. and Alterman Z., *Proc. Natl. Acad. Sci. USA* **43**, 998 (1957).
10. Ohwada T. and Sone Y., *Eur. J. Mech., B/Fluids*, **44** 389 (1992).
11. Gilbarg, D. and Paolucci, D., *J. Rat. Mech. Anal.* **2** 617 (1953).
12. Sone, Y. and Onishi Y., *J. Phys. Soc. Jpn.* **44**, 1981 (1978).
13. Ohwada T., *Phys. Fluids A* **5**, 217 (1993).
14. Ohwada, T., *Transp. Theo. Stat. Phys.* **29**, 495 (2000).
15. Sone, Y., Bardos, C., Golse, F., and Sugimoto H., *Eur. J. Mech. B-Fluids* **19**, 325 (2000).
16. Cercignani, C., *Meccanica* **5**, 7 (1970).
17. Sone, Y., Takata S., Sugimoto H., and Bobylev A.V., *Phys. Fluids* **8**, 628 (1996).